*34th EPS Conference on Plasma Phys. Warsaw, 2 - 6 July 2007 ECA Vol.**31F**, P-2.007 (2007)*

NUMERICAL SIMULATION OF INTENSE LASER-PLASMA INTERACTION USING AN EULERIAN VLASOV CODE

M. Shoucri

Institut de recherche d'Hydro-Québec (IREQ), Varennes, Québec, Canada, J3X 1S1

An eulerian code is used for the numerical solution of the one-dimensional relativistic Vlasov-Maxwell equations to study laser-plasma interaction, in the strongly relativistic regime [1]. The code applies a numerical scheme based on a two-dimensional advection technique, of second order accuracy in time-step, where the value of the distribution function is advanced in time by interpolating in two dimensions along the characteristics using a tensor product of cubic *B*-splines [2]. Both electrons and ions are included in the simulation. Non-periodic boundary conditions are used. At low laser intensities, in the weakly relativistic regimes, the instabilities reduce to Raman instabilities in which the electromagnetic (EM) wave decays into a resonant plasma wave and Stokes and also anti-Stokes waves. Recently, different couplings have been also discussed for intense laser lights [3,4], which include electron acoustic waves whose frequency is below the plasma frequency. In the present work, we consider the case of an intense pump of circularly polarized EM wave, with a quiver momentum $a_0 = p_{osc} / m_e c = 0.5$. The electrons are brought deeply to relativistic quiver velocities by interacting with the wave field, and laser light is subject to regimes of instabilities where the Fourier modes are strongly coupled.

The relevant equations

The one-dimensional Vlasov equations for the electron distribution function $f_e(x, p_{xe}, t)$ and ion distribution function $f_i(x, p_{xi}, t)$ are given by [1,2]:

$$\frac{\partial f_{e,i}}{\partial t} + m_{e,i} \frac{p_{xe,i}}{\gamma_{e,i}} \frac{\partial f_{e,i}}{\partial x} + (\mp E_x - \frac{m_{e,i}}{2\gamma_{e,i}} \frac{\partial a_\perp^2}{\partial x}) \cdot \frac{\partial f_{e,i}}{\partial p_{xe,i}} = 0 . \qquad (1)$$

Time *t* is normalized to ω_{pe}^{-1}, length is normalized to $l_0 = c\omega_{pe}^{-1}$, velocity and momentum are normalized respectively to the velocity of light *c*, and to $M_e c$. In our normalized units $m_e = 1$ for the electrons, and $m_i = M_e / M_i$ for the ions. The indices *e* and *i* refers to electrons and ions. In the direction normal to *x*, the canonical momentum written in our normalized units as $\vec{P}_{\perp e,i} = \vec{p}_{\perp e,i} \mp \vec{a}_\perp$ is conserved. $\vec{P}_{\perp e,i}$ can be chosen initially to be zero, so

that $\vec{p}_{\perp e,i} = \pm\vec{a}_\perp$ (the vector potential $\vec{a}_\perp$ is normalized to $M_e c/e$). $E_x = -\frac{\partial\varphi}{\partial x}$ and $\vec{E}_\perp = -\frac{\partial\vec{a}_\perp}{\partial t}$, $\gamma_{e,i} = \left(1+\left(m_{e,i}p_{xe,i}\right)^2+\left(m_{e,i}a_\perp\right)^2\right)^{1/2}$. The transverse EM fields E_y, B_z and E_z, B_y for the circularly polarized wave obey Maxwell's equations. With $E^\pm = E_y \pm B_z$ and $F^\pm = E_z \pm B_y$, we have:

$$(\frac{\partial}{\partial t} \pm \frac{\partial}{\partial x})E^\pm = -J_y \,.\;; \qquad (\frac{\partial}{\partial t} \mp \frac{\partial}{\partial x})F^\pm = -J_z \tag{2}$$

which are integrated along their vacuum characteristic $x=t$. In our normalized units :

$$\vec{J}_\perp = \vec{J}_{\perp e} + \vec{J}_{\perp i} \;;\; \vec{J}_{\perp e,i} = -\vec{a}_\perp m_{e,i}\int\frac{f_{e,i}}{\gamma_{e,i}}dp_{xe,i}, \text{ and } <1/\gamma_{e,i}>=\int\frac{f_{e,i}}{\gamma_{e,i}}dp_{xe,i}\,. \tag{3}$$

Results

The circularly polarized EM wave is excited at the left boundary x=0, where the forward propagating waves E^+ and F^- are excited in vacuum with $a_0 = e\,a_\perp/m_e c = 0.5$, and a wave frequency $\omega_0/\omega_{pe} = 1.3696$, $n_0/n_{crit} = \omega_p^2/\omega_0^2 \approx 0.533$ so that the density is above quarter critical. The results show the presence of stimulated electron acoustic wave scattering (SEAWS), similar to what has been described in [5]. Its spectrum is explained by a resonant three-wave parametric decay of the laser pump into the Stokes and anti-Stokes light sidebands and the EAW. Because of the high intensities, the Fourier modes are strongly coupled, with the growth of several neighbouring modes observed, and broad spectra around the maxima. Ion dynamics is included and shows in this early stage a strong modulation of the ion distribution function. Fig.(1) shows the frequency spectrum of the longitudinal plasma electric field E_x , with a broad peak at $\omega_{eaw} = 0.5478$, followed by peaks at 1.232,1.643,1.917,2.328,2.739. In Fig.(2) the plasma wavenumber spectrum has a broad peak at $k_{eaw} = 0.9587$, with other peaks at 0.5478,1.643,2.19,2.602,3.425. The dominant peaks at (ω_{eaw}, k_{eaw}) have been identified as an electron acoustic wave (note that in [5] the wave frequency ω_0 is used for normalization instead of ω_{pe}). Fig.(3) shows the frequency spectrum of the EM wave at a point in vacuum at the left boundary. The full curve is for the incident forward EM wave F^-,(it has a broad peak at $\omega_0 = 1.3696$), and the broken curve is for the backward F^+ wave (peaks at 0.8217,1.3696,1.78,2.054,2.739). Similar curves are obtained for E^+ and E^-. Fig.(4) shows the frequency spectrum of the forward EM wave

F^- inside the plasma at *x*=6.28 (full curve peaks at the pump frequency $\omega_0 = 1.3696$, the scattered Stokes frequency $\omega_s = 0.8217$, the anti-Stokes at 1.9174, and the frequencies 2.2, 2.739) , and the backward wave F^+ (broken curve, peaks at 0.8217,1.3696,2.602). The corresponding wavenumber spectrum of F^- has the dominant peak at k_0 = 1.095, and peaks at 0.1369, 0.5479, 1.75, 2.2, 2.6. The electromagnetic waves verify the relation $\omega_{0,s}^2 = \omega_p^2 < \gamma_e^{-1} > + k_{0,s}^2 c^2$, or in our normalized units $\omega_{0,s}^2 = < \gamma_e^{-1} > + k_{0,s}^2$. With $\omega_0 = 1.3696$ and $k_0 = 1.095$, we can derive $< \gamma_e^{-1} >= 0.6768$. The backward and forward scattered modes were driven with $k_s \approx 0$, so that $\omega_s \approx \sqrt{< \gamma_e^{-1} >} = 0.8226$. This corresponds very well to the forward and backward wave peaks at 0.8217 observed in Fig.(4). We can check the relation $\omega_0 = \omega_s + \omega_{eaw} \approx$ 0.8217+0.5478, and $k_0 = \pm k_s + k_{eaw} \approx k_{eaw}$. (The wavenumber spectra of the forward and backward wave F^- and F^+ show a peak at $k_s \approx 0.13696 = \Delta k$, but this is the lowest resolution, so that k_s could be in fact much smaller). Note that the frequency at 2.739 and wavenumber at 2.20 for the plasma waves in Figs.(1-2) are harmonics of (ω_0, k_0), as previously discussed in [2]. For the anti-Stokes coupling, we take from the spectrum of F^- $\omega_{as} = 1.9174$ (see Fig.(4)), $k_{as} = 1.75$ which satisfies $\omega_{as}^2 =< \gamma_e^{-1} > + k_{as}^2$, and which verifies $\omega_{as} = \omega_0 + \omega_{eaw} \approx 1.3696 + 0.5478$, $k_{as} = k_0 + k_{eaw} \approx$ 1.095+0.7 (note in Fig.(2) the broad peak at k_{eaw} =0.95). The electron density (initially equal to 1 in the central region) is shown in Fig.(5) at *t*= 71.4 (full curve), which shows spikes developing surrounded by depleted regions as the wave penetrates. The ion density (broken curve) remains essentially close to the original profile, although the phase-space contour plot in Fig.(8) of the ion distribution function shows a strong modulation. Fig.(6) shows the profile of the forward wave F^- (full curve) and backward wave F^+ (broken curve) at *t*= 71.4. The contour plot of the electron distribution function is shown in Fig.(7) at *t*= 71.4 and shows complex vortices developing.

References

[1] S. Guérin, G. Laval, P. Mora, J.C. Adam *et al*. Phys. Plasmas 2, 2807 (1995).
[2] M. Shoucri, 'The method of characteristics for the numerical solution of hyperbolic differential equations', in Computer Physics Research Trends (Ed. Silvan J. Bianco, Nova Science Publishers Inc.,NY) (2007); also in Comm.Nonl.Sci.Numer.Simul.(2007)
[3] D.J. Strozzi, E. Williams, A. Langdon, A. Bers Phys. Plasmas 14, 013104 (2007)
[4] N.J. Sircombe, T. Arber, R. Dendy Plasma Phys. Controlled Fusion 48, 1141 (2006)
[5] B. Li, S. Ishiguro, M. Skoric, M. Song, T. Sato J. Plasma Phys 72, 1257 (2006)

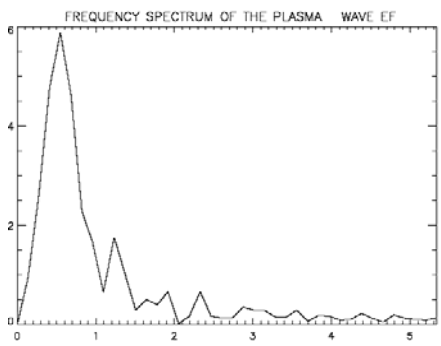

Fig.1

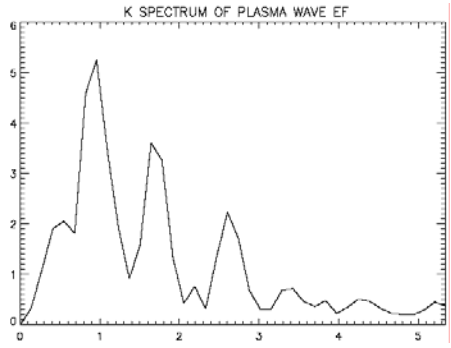

Fig.2

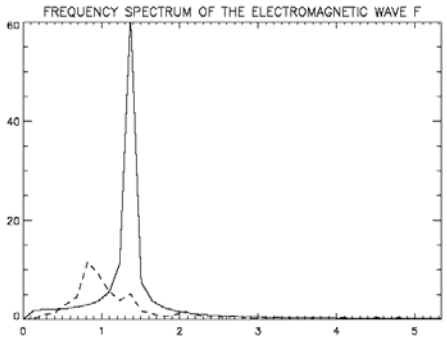

Fig.3

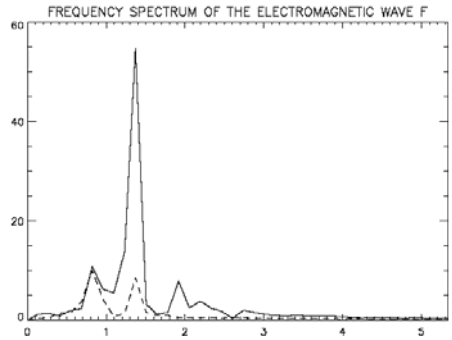

Fig.4

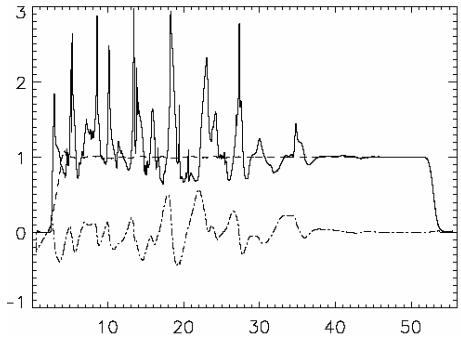

Fig.5

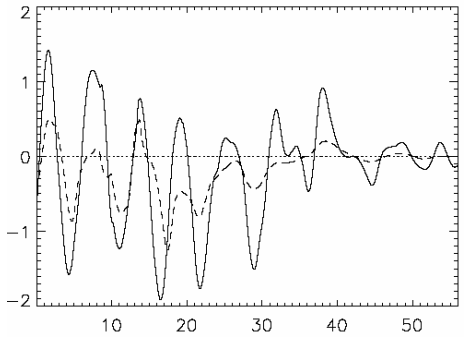

Fig.6

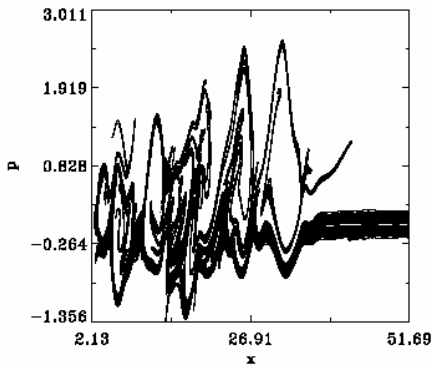

Fig.7 Contour plot of the Electron distribution function

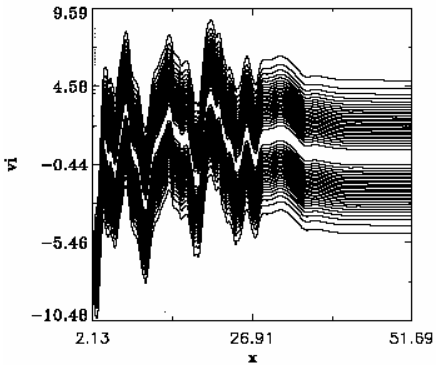

Fig.8 Contour plot of the ion distribution function, t= 71.4.